SEMARAK ILMU PUBLISHING

Journal of Advanced Research in Fluid Mechanics and Thermal Sciences

Journal homepage:
https://semarakilmu.com.my/journals/index.php/fluid_mechanics_thermal_sciences/index
ISSN: 2289-7879

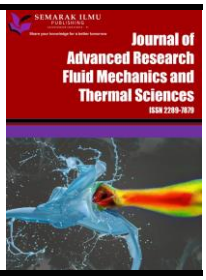

Effects of Thermal Diffusion and Diffusion Thermo on a Chemically Reacting MHD Peristaltic Transport of Bingham Plastic Nanofluid

Alaa Jaber Abuiyada[1,*], Nabil Tawfik Eldabe[2], Mohamed Yahya Abou-zeid[2], Sami Mohamed El Shaboury[1]

[1] Department of Mathematics, Faculty of Science, Ain Shams University, Cairo, Egypt
[2] Department of Mathematics, Faculty of Education, Ain Shams University, Cairo, Egypt

ARTICLE INFO

Article history:
Received 19 March 2022
Received in revised form 29 June 2022
Accepted 13 July 2022
Available online 7 August 2022

Keywords:
Peristalsis; Bingham plastic nanofluid; MHD; couple stresses; Soret and Dufour effects; Hall current; Joule heating; chemical reaction; radiation; Homotopy Perturbation Method (HPM)

ABSTRACT

In this work we investigated the solution of the peristaltic motion of Bingham plastic nanofluid through a vertical symmetric channel. The system is stressed by an external strong magnetic field to produce a hall currents. Moreover, we involved effects of Joule heating, radiation, chemical reaction and couple stresses. Further, we considered Soret and Dufour effects. This phenomenon is represented mathematically by a system of non-linear equations which describe the problem. We used the approximation of low Reynolds number and long-wavelength approximation to simplify the governing equations. Then, we used Homotopy perturbation method (HPM) to solve the equations. We sketched a graph for the influence of various parameters on velocity, temperature and nanoparticles concentration profiles and then discussed them physically. Finding revealed that an increase of Bingham number Bn and the regularization parameter of Bingham fluid m_1 decreases the velocity and increases the temperature, but radiation parameter R has an opposite relative to them. Also, we found that increasing of chemical reaction parameter γ reduces the nanoparticles concentration, whereas the reverse is the case when the reaction order n is increased.

1. Introduction

Couple stress fluids are a special case of non-Newtonian fluids in which the size of the fluid particles is taken into account. The study of couple stress fluids had major interest of the researchers due to its numerous industrial and scientific applications. In fact, couple stress fluid model is capable to describe different complex fluids like liquid crystals, polymeric suspensions with long chain molecules, infected urine, human and animal blood and many lubricants. Couple stress fluid model can also be also used to explain the flow of blood in arteries. Many researchers studied couple stress fluid for the peristaltic flow problems in different situation. Eldabe *et al.,* [1] studied the wall properties effect on the peristaltic motion of a coupled stress fluid with heat and mass

* *Corresponding author.*
E-mail address: alaaabuiyada2019@gmail.com

https://doi.org/10.37934/arfmts.98.1.2443

transfer through a porous medium. Homotopy perturbation method for couple stresses effect on MHD peristaltic flow of a non-Newtonian nanofluid investigated by Abou-zeid [2]. Alsaedi *et al.,* [3] investigated the peristaltic flow of couple stress fluid through uniform porous medium. Effects of slip and convective conditions on the peristaltic flow of couple stress fluid in an asymmetric channel through porous medium are discussed by Ramesh [4]. Also, Ramesh discussed the influence of heat and mass transfer on peristaltic flow of a couple stress fluid through porous medium in the presence of inclined magnetic field in an inclined asymmetric channel.

Researchers have given the topic of non-Newtonian fluids a lot of attention during the past few decades due to their great demand in several fields like rubber industry, manufacturing of paper production, polymer, production of petroleum, etc. Generally, when shear stress does not depend linearly on shear rate, the fluid is said to be non-Newtonian. Actually, applying force on the non-Newtonian fluids change their viscosity. Therefore, some of them become thicker and act like a solid, or in other cases they become faster than they were before. However, they return to their original state when the stress vanishes. Eldabe *et al.,* [6] studied the heat transfer of MHD non-Newtonian Casson fluid flow between two rotating cylinders. Electromagnetic and non-Darcian effects on a micropolar non-Newtonian fluid in boundary-layer flow with heat and mass transfer analyzed by Ouaf and Abou-zeid [7]. Eldabe and Mohamed [8] studied heat and mass transfer in hydromagnetic flow of the non-Newtonian fluid with heat source over an accelerating surface through a porous medium.

Nanofluids are a new category of fluids which are made up of nanometer-sized particles suspended in a base fluid. These nanoparticles are typically made up of non-metals such graphite and carbon nanotubes as well as metals, oxides, carbides, and nitrides. As a base fluid, biofluids, water, organic liquids, kerosene, lubricants, and polymeric solutions are typically employed. The objective of nanofluids is to achieve the highest level of thermal properties with the lowest level of concentration by uniform dispersion and stable nanoparticle suspension in the base fluids. As a result, when compared to base fluids, nanofluids have the ability to improve thermophysical properties such thermal conductivity, thermal diffusivity, viscosity, and convective heat transfer coefficients.

Non-Newtonian nanofluids are widely encountered in several industrial and technology applications, such as melts of polymers, biological solutions, paints, asphalts, tars and glues. Therefore, the study of non-Newtonian nanofluids had attracted many researchers. Numerous industrial and technological applications, including melts of polymers, biological solutions, paints, asphalts, tars, and glues are example of frequently used non-Newtonian nanofluids. As a result, several researchers became interested in studying non-Newtonian nanofluids. Eldabe *et al.,* [9] studied instantaneous thermal-diffusion and diffusion-thermo effects on Carreau nanofluid flow over a stretching porous sheet. Mohamed and Abou-zeid [10] investigated MHD peristaltic flow of micropolar Casson nanofluid through a porous medium between two co-axial tubes. Eldabe *et al.,* [11] analyzed the effect of induced magnetic field on non-Newtonian nanofluid Al_2O_3 motion through boundary-layer with gyrotactic microorganisms. Thermal diffusion and diffusion thermo effects on Magnetohydrodynamics transport of non-Newtonian nanofluid through a porous media between two wavy co-axial tubes studied by Eldabe *et al.,* [12]. Also, Eldabe *et al.,* [13] analyzed ohmic and viscous dissipation effects on micropolar non-Newtonian nanofluid Al_2O_3 flow through a non-Darcy porous media. Implicit homotopy perturbation method for MHD non-Newtonian nanofluid flow with Cattaneo-Christov heat flux due to parallel rotating disks investigated by Abou-zeid [14]. Eldabe *et al.,* [15] studied thermal diffusion and diffusion thermo effects of Eyring- Powell nanofluid flow with gyrotactic microorganisms through the boundary layer.

Bingham plastic fluids is an example of non-Newtonian viscoplastic fluids. The most important characteristics of Bingham plastic fluids is their yield stress which defines the point above which flow occurs. Shear stress for Bingham Plastic fluids depends linearly on strain. So, Bingham plastic fluid cannot preserve a velocity gradient unless the magnitude of the shear stress is higher than its yield stress. Therefore, the motion of Bingham plastic fluid at a stress level lower than its yield stresses is very similar to that of a rigid body, but it flows like a viscous fluid when the stress level becomes high. Paint, toothpaste, printing ink, clay, drilling mud, molten liquid crystalline polymers, foams and food articles like margarine, mayonnaise, molten chocolate, yoghurts and ketchup are some typical examples of Bingham plastic fluids. Moreover, Bingham plastics such as cement mortar, slurries and suspensions are widely used in hydraulic and civil engineering. Therefore, many researches have been done to analyze the effects of Bingham plastic nanofluid in different situations. Eldabe *et al.,* [16] examined the wall properties and Joule heating effects on MHD peristaltic transport of Bingham non-Newtonian nanofluid. Eldabe *et al.,* [17] discussed Cattaneo-Christov heat flux effect on MHD peristaltic transport of Bingham Al_2O_3 nanofluid through a non-Darcy porous medium. MHD peristaltic transport of Bingham blood fluid with heat and mass transfer through a non-uniform channel examind by Eldabe *et al.,* [18]. Ismael *et al.,* [19] discussed the activation energy and chemical reaction effects on MHD Bingham nanofluid flow through a non-Darcy porous media. Ibrahim *et al.,* [20] investigated the activation energy and chemical reaction effects on MHD Bingham nanofluid flow through a non-Darcy porous media.

The peristaltic flows of non-Newtonian nanofluids have received considerable attentions due to to extensive uses in physiology and industry. A spontaneous process of area contraction and expansion along the length of the channel is referred to as peristalsis. Many body parts, including the stomach, gastrointestinal tract, and small intestines, exhibit peristalsis. The movement of food bolus in the digestive system, the motion of chyme in the gastrointestinal tract, the movement of an ovum in a fallopian tube, the transport of lymph in lymphatic vessels, the passage of bile from the gall bladder to the duodenum, the flow of urine from the kidneys to the bladder, etc. Moreover, peristalsis plays an important role in designing of numerous devices like heart lung machines, dialysis machines and blood pump machines that pump the blood during many biomedical processes. Also, some worms also move themselves forward using the peristaltic process. The peristaltic flow problem has been studied in a number of contexts due to its wide range of applications. Eldabe *et al.,* [21] studied the homotopy perturbation approach for ohmic dissipation and mixed convection effects on non-Newtonian nanofluid flow between two co-axial tubes with peristalsis. Mustafa *et al.,* [22] obtained the slip effects on peristaltic motion of nanofluid in a channel with wall properties. In fact, Peristaltic flow with heat and mass transfer has also various applications in geophysical engineering and geothermal. Therefore, the importance of heat exchange with peristaltic mechanism cannot be neglected due to its applications in solar ponds, lubrication technology, diffusion of different nutrients from blood, drying technology, a dynamic of lakes, haemodialysis and nuclear reactors. Eldabe *et al.,* [23] analyzed the effect of heat and mass transfer on Casson fluid flow between two co-axial tubes with peristalsis. Eldabe and Abou-zeid [24] investigated radially varying magnetic field effect on peristaltic motion with heat and mass transfer of a non-Newtonian fluid between two co-axial tubes. Mansour and Abouzeid [25] analyzed heat and mass transfer effect on non-newtonian fluid flow in a non-uniform vertical tube with peristalsis. Homotopy perturbation method for creeping flow of non-Newtonian Power-Law nanofluid in a nonuniform inclined channel with peristalsis stuided by Abou-zeid and Mohamed [26]. Peristaltic flow of Herschel Bulkley nanofluid through a non-Darcy porous medium with heat transfer under slip condition discussed by Eldabe *et al.,* [27]. A semianalytical technique for MHD peristalsis of pseudoplastic nanofluid with temperature dependent viscosity investigated by Eldabe *et al.,* [28].

Also, Eldabe *et al.,* [29] investigated MHD peristaltic flow of non-Newtonian power-law nanofluid through a non-Darcy porous medium inside a non-uniform inclined channel.

Several investigations have been carried-out to examine the effect of chemical reaction on heat and mass transfer problems due to its importance in hydrometallurgical industries and chemical technology including the production of pulp and insulated cables as well as the curing of polymers, cleaning, and chemical processing of materials. Chemical reaction order may be of first order or higher. Eldabe *et al.,* [30] studied the electromagnetic steady motion of Casson fluid with heat and mass transfer through porous medium past a shrinking surface. Ouaf *et al.,* [31] investigated entropy generation and chemical reaction effects on MHD non-Newtonian nanofluid flow in a sinusoidal channel. Eldabe *et al.,* [32] studied magnetohydrodynamic non-Newtonian nanofluid flow over a stretching sheet through a non-Darcy porous medium with radiation and chemical reaction.

The impact of Hall currents on the flow is worth studying due to their significant effects on the direction and the magnitude of the current density and accordingly on the term of the magnetic force. The Hall effect principle is used to assess the performance of several equipment, including heat exchangers and power generators. The influence of Hall current becomes significant when the Hall parameter is high. In fact, this condition develops as a result of a high magnetic field or a low collision frequency since the Hall effect parameter is defined as the ratio between the electron-cyclotron frequency and the electron-atom collision frequency. Many researches have been done to analyse the effect of Hall currents on peristaltic flow. Eldabe *et al.,* [33] studied semi-analytical treatment of Hall current effect on peristaltic flow of Jeffery nanofluids. Eldabe *et al.,* [34] investigated the effect of induced magnetic field on non-Newtonian nanofluid $\mathrm{Al_2O_3}$ motion through boundary-layer with gyrotactic microorganisms. Asghar *et al.,* discussed Hall and ion slip effects on peristaltic flow and heat transfer analysis with Ohmic heating [35]. Elshehawey *et al.,* [36] studied chebyshev finite difference method for the effects of Hall and ion-slip currents on magnetohydrodynamic flow with variable thermal conductivity. Nowar [37] investigated the peristaltic flow of a nanofluid under the effect of Hall current and porous Medium. Numerical analysis for MHD peristaltic transport of Carreau–Yasuda fluid in a curved channel with Hall effects investigated by Abbasi *et al.,* [38].

The purpose of this study is to extend the work of Akbar *et al.,* [39] by including chemical reaction, Soret and Dufour effects, couple stresses and Joule heating on the peristaltic transport of MHD Bingham plastic nanofluid. We simplified the governing equations; continuity, momentum, energy and nanoparticle concentration, by using the long wavelength and low Reynolds number approximation. Then, we used the Homotopy perturbation method (HPM) to solve the simplified equations. We also observed the Brownian motion and thermophoresis effects. Moreover, we plotted graphs to demonstrate the effects of some embedded parameters on the behavior of the variable of state such as velocity, temperature and nanoparticle concentration, and then we discussed them physically. Furthermore, we obtained graphs for entropy generation number, Nusselt number, Sherwood number and heat transfer coefficient.

2. Mathematical Formulation

We assumed a peristaltic flow of MHD Bingham plastic nanofluid in a two-dimensional symmetric vertical channel of uniform thickness $2\mathrm{d}$. The X-axis lies along the channel axis, while the Y-axis is perpendicular to it. Also, the velocity components U and V lie along X and Y directions, respectively. Chemical reaction, Brownian motion, thermophoresis, viscous dissipation, Joule

heating, radiation and couple stresses effects are involved. The geometry of the waves surface is described as

$$y = h_1(X,t) = \left[d + a\,cos\frac{2\pi}{\lambda}(X - ct)\right] \tag{1}$$

$$y = h_2(X,t) = -\left[d + a\,cos\frac{2\pi}{\lambda}(X - ct)\right] \tag{2}$$

where $\mathrm{h_1(X,t)}$ and $\mathrm{h_2(X,t)}$ are the right and left walls respectively. Here, we assume the nanofluid to be electrically conducting in the presence of a uniform magnetic field $\mathrm{B} = (0,0,\mathrm{B_0})$ applied in the z-direction. The current density J including the Hall effect and ignoring the ion-slip effects can be expressed as [40, 41]

$$J = \sigma_f(E + V \times B) - \frac{\sigma}{en_e}(J \times B) \tag{3}$$

where σ_f is the electric conductivity of the fluid E is the electric field, V is the vector velocity, e is the electric charge and n_e is the number density of electrons. For small Reynolds magnetic number with no polarization voltage and no surface charge, the induced magnetic field and electric field are ignored; therefore, Eq. (3) may be written as follows

$$J = \frac{\sigma_f\, B_0}{1 + m^2}[\,(V + m\,U)\hat{\imath} + (mV - \,U)\hat{\jmath}\,] \tag{4}$$

where $m = \frac{\sigma B_0}{en_e}$ is the Hall parameter. Through Eq. (4) we have

$$F = J \times B = \frac{\sigma_f\, B_0^2}{1 + m^2}[\,(mV - \,U)\hat{\imath} - (V + mU)\hat{\jmath}\,] \tag{5}$$

$$\frac{J.J}{\sigma_f} = \frac{\sigma_f\, B_0^2}{1 + m^2}(V^2 + U^2) \tag{6}$$

The term $J \times B$ represents the Lorentz force per unit volume and the term $\frac{J.J}{\sigma_f}$ represents Joule heating. The constitutive equation that obeys the behaviour of incompressible Bingham plastic fluid is regularised as [42-44]

$$S = \eta_p\,\bar{\bar{\dot{\gamma}}} \tag{7}$$

$$S = \left(\mu_p + \frac{\tau_y}{|\dot{\gamma}|}[1 - exp(-m_1|\dot{\gamma}|)]\right)\bar{\bar{\dot{\gamma}}} \qquad for\ \ \tau \geq \tau_y \tag{8}$$

$$S = \bar{\bar{\dot{\gamma}}} = 0 \qquad for\ \ \tau < \tau_y \tag{9}$$

where S refers to the extra stress tensor, $\dot{\bar{\bar{\gamma}}} = (\nabla \mathrm{v} + \nabla^T \mathrm{v})$ represents the rate of stress tensor, $|\dot{\gamma}| = \left[\frac{1}{2}\dot{\bar{\bar{\gamma}}} : \dot{\bar{\bar{\gamma}}}\right]^{\frac{1}{2}}$ express the magnitudes of the rate of deformation, τ_y called the yield stress and m_1 is the regularization parameter which controls the exponential growth of stress. Actually, $m_1 = 0$ refers to the Newtonian fluid behaviour, whereas $m_1 \to \infty$ mimics the ideal Bingham plastic model. The non-dimensional viscosity for Bingham plastic fluid can be expressed by using the dimensionless variables $c, d_1, \mu_p(c/d_1)$ and d/c for velocity, length, shear stress and time respectively as follows

$$\eta_p = \left(1 + \frac{Bn}{|\dot{\gamma}|}[1 - exp(-m_1|\dot{\gamma}|)]\right) \tag{10}$$

where $Bn = \frac{\tau_y\, d_1}{\mu_p\, c}$ called the Bingham number.

The equations that govern the Magnetohydrodynamic Bingham plastic nanofluid in the presence of Sorte and Dufour effects, viscous dissipation radiation, couple stresses and chemical reaction are described as

$$\frac{\partial U}{\partial X} + \frac{\partial V}{\partial Y} = 0 \tag{11}$$

$$\rho_f\left(\frac{\partial U}{\partial t} + U\frac{\partial U}{\partial X} + V\frac{\partial U}{\partial Y}\right) = -\frac{\partial P}{\partial X} + \frac{\partial S_{XX}}{\partial X} + \frac{\partial S_{XY}}{\partial Y} + g(\rho\beta)_f(T - T_0) + g(\rho\beta)_f(C - C_0) - \frac{\sigma B_0^2}{1 + m^2}(U - mV) - \eta_1\frac{\partial^4 U}{\partial Y^4} \tag{12}$$

$$\rho_f\left(\frac{\partial V}{\partial t} + U\frac{\partial V}{\partial X} + V\frac{\partial V}{\partial Y}\right) = -\frac{\partial P}{\partial Y} + \frac{\partial S_{XY}}{\partial X} + \frac{\partial S_{YY}}{\partial Y} - \frac{\sigma B_0^2}{1 + m^2}(V + mU) - \eta_1\frac{\partial^4 V}{\partial Y^4} \tag{13}$$

$$(\rho c)_f\left(\frac{\partial T}{\partial t} + U\frac{\partial T}{\partial X} + V\frac{\partial T}{\partial Y}\right) = \kappa_f\left(\frac{\partial^2 T}{\partial X^2} + \frac{\partial^2 T}{\partial Y^2}\right) - \frac{\partial q_r}{\partial Y} + \Phi + \left(S_{XX}\frac{\partial U}{\partial X} + S_{XY}\left(\frac{\partial U}{\partial Y} + \frac{\partial V}{\partial X}\right) + S_{YY}\frac{\partial V}{\partial Y}\right) + (\rho c)_p\left[D_B\left(\frac{\partial C}{\partial X}\frac{\partial T}{\partial X} + \frac{\partial C}{\partial Y}\frac{\partial T}{\partial Y}\right) + \frac{D_T}{T_m}\left(\left(\frac{\partial T}{\partial X}\right)^2 + \left(\frac{\partial T}{\partial Y}\right)^2\right)\right] + \frac{D_B K_T}{c_s}\left(\frac{\partial^2 C}{\partial X^2} + \frac{\partial^2 C}{\partial Y^2}\right) + \frac{\sigma_f B_0^2}{(1 + m^2)}(U^2 + V^2) \tag{14}$$

$$\frac{\partial C}{\partial t} + U\frac{\partial C}{\partial X} + V\frac{\partial C}{\partial Y} = D_B\left(\frac{\partial^2 C}{\partial X^2} + \frac{\partial^2 C}{\partial Y^2}\right) + \left(\frac{D_T + D_B K_T}{T_m}\right)\left(\frac{\partial^2 T}{\partial X^2} + \frac{\partial^2 T}{\partial Y^2}\right) - k_1(C - C_0)^n \tag{15}$$

Here, q_r is the radiative heat flux which gives by [45]

$$q_r = \frac{-4\sigma^*}{3k_R}\frac{\partial T^4}{\partial Y} \tag{16}$$

where σ^*, k_R represent the Stefan-Boltzmann constant and the mean absorption coefficient, respectively. We assume that the difference of temperature within the flow is sufficiently small as the term T^4 in Taylor series about temperature T_0 which can be expressed as follows:

$$T^4 = T_0^4 + 4\,T_0^3(T - T_0) + 6\,T_0^2\,(T - T_0)^2 + \cdots \tag{17}$$

By neglecting higher order terms in Eq. (17) beyond the first order in $(T - T_0)$, we obtain

$$T^4 \cong 4\,T_0^3 T - 3T_0^4 \tag{18}$$

Substituting Eq. (18) into Eq. (16), we get

$$q_r = -\frac{16\,\sigma^* T_0^3}{3k_R}\frac{\partial T}{\partial Y} \tag{19}$$

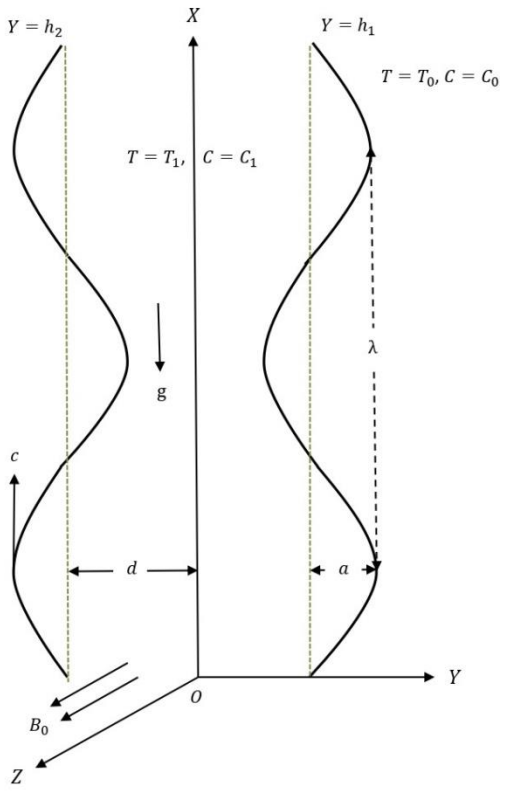

Fig. 1. Geometry of the problem

Transformation between laboratory and moving frames is given as

$$y = Y, x = X - ct, p(x,y) = P(X,Y,t), u = U - c, v = V(x,y,t), T(x,y) = T(X,Y,t),$$
$$C(x,y) = C(X,Y,t) \tag{20}$$

where (u, v) are the components of velocity in wave frame (x, y). Defining the following non-dimensional quantities

$$u^* = \frac{u}{c}\,, v^* = \frac{v}{c\delta}\,, x^* = \frac{x}{\lambda}\,, y^* = \frac{y}{d}\,, t^* = \frac{ct}{\lambda}\,, p^* = \frac{d^2p}{c\lambda\mu}\,, \theta = \frac{T - T_0}{T_1 - T_0}\,, \phi = \frac{C - C_0}{C_1 - C_0} \tag{21}$$

Since Reynolds number is small for the fluid mechanics in small intestine, we assumed Reynolds number to be small $(Re \approx 0)$. Moreover, we assumed that the wave number $\delta = (d/\lambda)$ is small $(\delta \approx 0)$ under the assumption of the long-wavelength which states that the wavelength λ of the peristaltic wave is considerably large comparing with the half width of the channel d. Applying the transformation between laboratory and moving frames in Eq. (20) and the low Reynolds number and long-wavelength approximation, the Eq. (11) to Eq. (15) are transformed to:

$$\frac{\partial u}{\partial x} + \frac{\partial v}{\partial y} = 0 \tag{22}$$

$$\frac{\partial P}{\partial x} = (1 + Bn\, m_1)\frac{\partial^2 u}{\partial y^2} - m_1^2\, Bn\, \frac{\partial u}{\partial y}\frac{\partial^2 u}{\partial y^2} + Gr\theta + Gc\phi - \frac{M^2}{1 + m^2}(u + 1) - \frac{1}{\gamma_1^2}\frac{\partial^4 u}{\partial y^4} \tag{23}$$

$$\frac{\partial P}{\partial y} = 0 \tag{24}$$

$$\left(1 + \frac{4}{3}R\right)\frac{\partial^2 \theta}{\partial y^2} + Br\,(1 + Bn\, m_1)\left(\frac{\partial u}{\partial y}\right)^2 - \frac{m_1^2}{2}\, Br\, Bn\, \left(\frac{\partial u}{\partial y}\right)^3 + Nb\, Pr\frac{\partial \phi}{\partial y}\frac{\partial \theta}{\partial y} + Nt\, Pr\left(\frac{\partial \theta}{\partial y}\right)^2 + Du\, Pr\frac{\partial^2 \phi}{\partial y^2} + \frac{M^2}{1 + m^2} Br\,(u + 1)^2 + \varepsilon = 0 \tag{25}$$

$$\frac{\partial^2 \phi}{\partial y^2} + \left(\frac{Nt}{Nb} + Sc\, Sr\right)\frac{\partial^2 \theta}{\partial y^2} - \gamma\, Sc\, \phi^n = 0 \tag{26}$$

Dimensionless boundary conditions are given as [39, 46]

$$u = 0\,, \frac{\partial u}{\partial y} = 0\,, \theta = 1, \phi = 1 \qquad at \quad y = 0 \tag{27}$$

$$\frac{\partial^2 u}{\partial y^2} = 0\,, u + \beta_1 \frac{\partial u}{\partial y} = -1\,, \gamma_2 \theta + \frac{\partial \theta}{\partial y} = 0\,, \gamma_3 \phi + \frac{\partial \phi}{\partial y} = 0 \qquad at \quad y = h_1 \tag{28}$$

where

$$S_{ij}^{*}=\frac{d}{c\mu}S_{ij}\,,Re=\frac{\rho_f cd}{\mu}\,,\delta=\frac{d}{\lambda}\,,M=\sqrt{\frac{\sigma}{\mu}}B_0 d\,,Pr=\frac{\mu c_p}{k}\,,Ec=\frac{c^2}{c_{p(T_1-T_0)}}\,,Br=Ec\,Pr\,,$$
$$Sc=\frac{\nu}{D_B}\,,Nb=\frac{\tau_1\,D_B}{\nu}(C_1-C_0),\;\;Nt=\frac{\tau_1\,D_T}{\nu\,T_m}(T_1-T_0)\,,$$
$$Du=\frac{D_B\,K_T\,(C_1-C_0)}{\mu c_s c_f\;(T_1-T_0)}\,,Sr=\frac{D_B\,K_T\,(T_1-T_0)}{T_m\,(C_1-C_0)}\,,\gamma=\frac{k_1\,d^2}{\nu}\,,\epsilon=\frac{a}{d}\,,$$
$$Gr=\frac{\rho_f g\beta_f\,d^2(T_1-T_0)}{c\mu}\,,Gc=\frac{\rho_f g\beta_f d^2(C_1-C_0)}{c\mu}\,,\gamma_1=\sqrt{\frac{\mu}{\eta_1}}d\,,$$
$$R=\frac{4\sigma^{*}T_0^3}{k_f k_R} \tag{29}$$

and the x-y component of the extra stress tensor of the Bingham plastic fluid is given as

$$S_{xy}=(1+Bn\,m_1)\frac{\partial u}{\partial y}-\frac{m_1^2\,Bn}{2}\left(\frac{\partial u}{\partial y}\right)^2 \tag{30}$$

3. Method of Solution

3.1 Homotopy Perturbation Method (HPM)

To solve the equations of velocity, temperature, and nanoparticle concentration, we employed a semi-analytical method known as the Homotopy perturbation method (HPM). This method is a combination of the classical perturbation technique and the Homotopy technique. This analytical method keeps all the advantages of the traditional perturbation methods while eliminating their drawbacks. HPM recommends to write Eq. (23), Eq. (25) and Eq. (26) as follows [47, 48]

$$\begin{aligned}(1-p)&\left(\frac{1}{\gamma_1^2}\frac{\partial^4 u}{\partial y^4}-\frac{1}{\gamma_1^2}\frac{\partial^4 u_0}{\partial y^4}\right)\\&+p\left(\frac{1}{\gamma_1^2}\frac{\partial^4 u}{\partial y^4}-(1+Bn\,m_1)\frac{\partial^2 u}{\partial y^2}+m_1^2\,Bn\,\frac{\partial u}{\partial y}\frac{\partial^2 u}{\partial y^2}-Gr\theta-Gc\phi\right.\\&\left.+\frac{M^2}{1+m^2}(u+1)-\frac{\partial P}{\partial x}\right)=0\end{aligned} \tag{31}$$

$$\begin{aligned}(1-p)&\left(\left(1+\frac{4}{3}R\right)\frac{\partial^2\theta}{\partial y^2}-\left(1+\frac{4}{3}R\right)\frac{\partial^2\theta_0}{\partial y^2}\right)\\&+p\left(\left(1+\frac{4}{3}R\right)\frac{\partial^2\theta}{\partial y^2}+Br\,(1+Bn\,m_1)\left(\frac{\partial u}{\partial y}\right)^2-\frac{m_1^2}{2}\,Br\,Bn\,\left(\frac{\partial u}{\partial y}\right)^3+Nb\,Pr\frac{\partial\phi}{\partial y}\frac{\partial\theta}{\partial y}\right.\\&\left.+Nt\,Pr\left(\frac{\partial\theta}{\partial y}\right)^2+Du\,Pr\frac{\partial^2\phi}{\partial y^2}+\frac{M^2}{1+m^2}Br\,(u+1)^2+\varepsilon\right)=0\end{aligned} \tag{32}$$

$$(1-p)\left(\frac{\partial^2\phi}{\partial y^2}-\frac{\partial^2\phi_0}{\partial y^2}\right)+p\left(\frac{\partial^2\phi}{\partial y^2}+\left(\frac{Nt}{Nb}+Sc\ Sr\right)\frac{\partial^2\theta}{\partial y^2}-\gamma\ Sc\ \phi^n\right)=0 \tag{33}$$

The initial approximations u_0, θ_0 and ϕ_0 can be written as the following

$$u_0=\frac{\left(\frac{r^3}{6}-h\frac{r^2}{2}\right)}{\left(\frac{h^3}{3}+\frac{\beta_1 h^2}{2}\right)},\theta_0=1-\left(\frac{\gamma 2\ r}{\gamma 2\ h\ +\ 1}\right),\phi_0=1-\left(\frac{\gamma 3\ r}{\gamma 3\ h\ +1}\right) \tag{34}$$

and we define u, θ and ϕ as follows

$$(u,\theta,\phi)=(u_0,\theta_0,\phi_0)+p\ (u_1,\theta_1,\phi_1)+p^2\ (u_2,\theta_2,\phi_2)+\cdots \tag{35}$$

where $p\in[0,1]$ is the embedding parameter. Here, we obtained the solutions of velocity, temperature and nanoparticle concentration when $p=1$ as follows

$$u(x,y)=c_1\ +c_2y+c_3y^2+c_4y^3+c_5y^4+c_6y^5+c_7\ y^6+c_8y^7 \tag{36}$$

$$\theta(x,y)=c_9+c_{10}\ y+c_{11}y^2+c_{12}\ y^3+c_{13}\ y^4+c_{14}\ y^5+c_{15}\ y^6+c_{16}\ y^7+c_{17}\ y^8 \tag{37}$$

$$\phi(x,y)=c_{18}+c_{19}\ y+c_{20}y^2+c_{21}\ y^3 \tag{38}$$

Here, c_1 - c_{21} are not included in order to save space, but they are available upon request. Also, we defined the skin friction coefficient τ_{xy}, heat transfer coefficient $Z(x)$, Nusselt number Nu and Sherwood number Sh at the right wall of the channel as follows [49]

$$\tau_{xy}=\left(1+Bn\ m_1\ \left(1-\frac{m_1}{2}\right)\right)\left(\frac{\partial u}{\partial y}\right)_{y\to h_1},Z(x)=\frac{\partial h_1}{\partial x}\left(\frac{\partial\theta}{\partial y}\right)_{y\to h_1},Nu=-\left(\frac{\partial\theta}{\partial y}\right)_{y\to h_1},$$
$$Sh=-\left(\frac{\partial\phi}{\partial y}\right)_{y\to h_1} \tag{39}$$

we obtained the above expressions by substituting Eq. (36) - (38) into Eq. (39), and then we used the software Mathematica package to evaluate them numerically for different parameters of the given problem.

3.2 Convergence of Homotopy Perturbation Method

Assume that the solution of Eq. (31) - (33) can be written as a power series as follows

$$n(r,P)=n_0+Pn_1+P^2n_2+\cdots \tag{40}$$

where, n is one of the physical quantities *w*, θ , and ϕ . Setting $P=1$, we obtain the semi-analytical solution of Eq. (31) - (33) as follows

$$n=\lim_{p\to 1}(n^0+Pn^1+P^2n^2+\ldots) \tag{41}$$

The series of Eq. (31) - (33) is convergent for most of all cases. Similarly, suppose that the solution of equations (36) - (38) can be written as a power series as follows

$$m(r,P) = m_0 + Pm_1 + P^2 m_2 \ldots \tag{42}$$

where, m is one of the physical quantities u, θ , and ϕ . Putting $P = 1$we obtain the semi-analytical solution of Eq. (36) - (38) as follows

$$m = \underset{p\to 1}{Lim}(m^0 + Pm^1 + P^2 m^2 + \ldots..) \tag{43}$$

The series of Eq. (36) - (38) is convergent for most of all cases.

4. Entropy Generation

Entropy generation plays a great role in increasing the efficiency of the system thermal. Entropy generation Exhibited areas of a physical model for the systems in the presents of large heat dissipation. MHD is also such non-ideal effects that causes an increase of the whole volumetric entropy of the system. For an MHD Bingham plastic nanofluid the dimensionless entropy generation is given as [50]

$$Ns = \left(\frac{\partial\theta}{\partial y}\right)^2 + \frac{1}{\left(1+\frac{4}{3}R\right)}\left[Br\,(1+Bn\,m_1)\left(\frac{\partial u}{\partial y}\right)^2 - \frac{m_1^2}{2}\,Br\,Bn\,\left(\frac{\partial u}{\partial y}\right)^3 + Nb\,Pr\frac{\partial\phi}{\partial y}\frac{\partial\theta}{\partial y}\right.$$
$$\left. + Nt\,Pr\left(\frac{\partial\theta}{\partial y}\right)^2 + Du\,Pr\frac{\partial^2\phi}{\partial y^2} + \frac{M^2}{1+m^2}Br\,(u+1)^2 + \varepsilon\right] \tag{44}$$

5. Results and Discussion

The main goal of this investigation is to observe the effect of some parameters of interest of Bingham plastic nanofluid on the velocity, temperature and nanoparticle concentration profiles. Moreover, graphs for the impact of various parameters on heat transfer coefficient, Nusselt number, Sherwood number and entropy generation are sketched. Furthermore, we provided a relevant physical explanation. We plotted the graphs of this study by taking $x = 0.2,\ \epsilon = 0.1$, $t = 0.1$ and $dp/dx = 5$. Also, the standard values of the involved parameters are $m_1 = Bn = Gr = Gc = Nt = Nb = Du = M = Sc = n = 1,\ Br = \beta_1 = 0.2,\ \gamma_1 = 8,\ m = \gamma = \gamma_2 = \gamma_3 = 0.1,\ Sr = R = 0.5$ and $Pr = \varepsilon = 2$.

The variation of the velocity distribution u versus the normal axis y with different values of the regularization parameter of Bingham fluid m_1 and Grashof number Gr is given in Figure 2 and Figure 3, respectively. These figures show a reduce in the velocity distribution u by increasing m_1, while it enhances by increasing Gr. Moreover, it is clear from these figures that as the normal axis y increasing, the difference of the velocity u for various values of m_1 and Gr becomes lower and arrives the lowest value, after which is increases. Further, we can observe from these figures that the lowest value of u decreases with the increase of m_1, while it increases as Gr increasing. Physically, increasing the plasticity of the fluid enhances the friction force of the fluid which reduces the velocity. In fact, $m_1 = 0$ refers to the Newtonian fluid behaviour, whereas $m_1 \to \infty$ mimics the ideal Bingham plastic model. The effect of Bn, m and γ_1 on the velocity distribution u along the normal axis y is found to be similar to the effect of m_1 that is given in Figure 2. Also, we found out that the influence of the parameters Br, γ, γ_2, γ_3, Sc, Gc, ε, R, Nt, Nb and M on the velocity

distribution u is similar to the effect of Gr that is shown in Figure 3, but the obtained curves for these parameters are closer to each other when compared with the curves that obtained in Figure 2 and Figure 3. Note that these figures are not provided here to prevent any type of duplication. Figure 4 depicts the influence of the velocity slip parameter β_1 on the velocity distribution u. We noticed from Figure 4 that the velocity distribution u increases as β_1 increases, when $y > 0.65$ there is a considerable difference between the graphs. By increasing the normal axis y, the difference of the velocity u for several values of β_1 becomes lower and gets to the minimum value, after which is increases. It is clear that the minimum value of u decreases by enhancing the value of β_1.

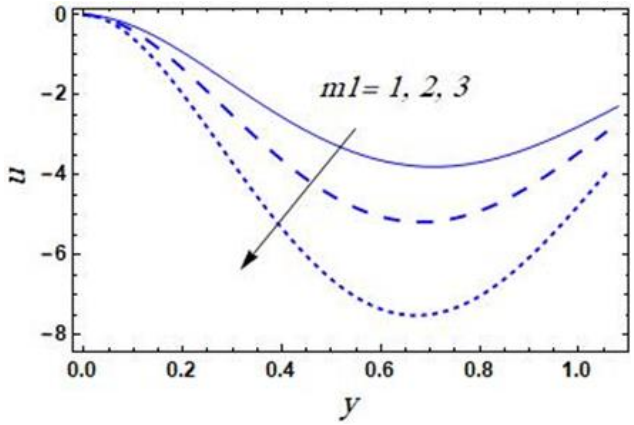

Fig. 2. Variation of m_1 on u versus y

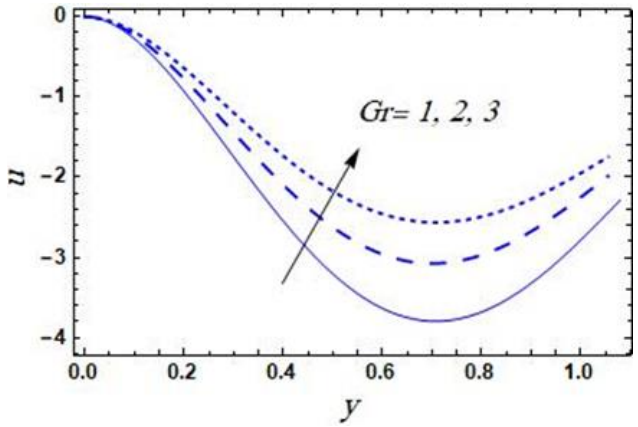

Fig. 3. Variation of Gr on u versus y

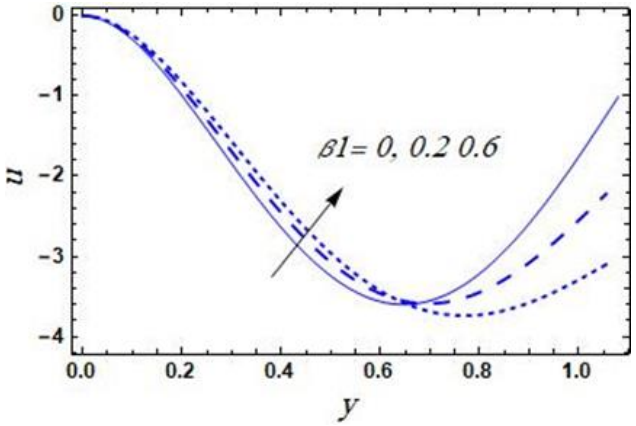

Fig. 4. Variation of β_1 on u versus y

Figure 5 and Figure 6 represent the behavior of the temperature distribution θ versus the normal axis y for various values of the dimensional heat generation/absorption parameter ε and the radiation parameter R, respectively. These figures show that the temperature distribution θ is enhance by increasing ε, while it decreases by increasing the value of R. In fact, radiation causes a lack of energy which causes a reduction in temperature, whereas heat generation enhances the energy which increase the temperature. Moreover, as the normal axis y increases, the change of the temperature θ for different values of ε, and R becomes greater and ends up with the maximum value at the right wall. Note that the maximum value of θ near the right wall increases as the value of ε increases, whereas it decreases by increasing the value of R. The findings in Figure 5 and Figure 6 are in a good agreement with those found by Akbar *et al.,* [39]. We observed that the influence of m_1, Bn, Br and M on the temperature distribution θ versus y is similar to the effect of ε that is captured in Figure 4. Further, we found out that the effects of m, β_1, γ, γ_1, γ_2, γ_3, Sc, Gr and Gc on

the temperature distribution θ are similar to the effect of R that is given in Figure 6. But, the obtained curves for γ, γ_1, γ_3, Sc, Gr and Gc are closer to each other comparing with those captured in Figure 5 and Figure 6. Note that these figures are not given here to save space. In addition, the variation of the temperature distribution θ versus the normal axis y for different values of Brownian motion parameter Nb and the thermophoresis parameter Nt is captured in Figure 7 and Figure 8, respectively. We observed that the influence of Nb and Nt on the temperature distribution θ is similar to the effect of ε that given is in Figure 5, but the obtained curves are closer to each other comparing with those in Figure 5. Physically, an enhancement in the Brownian motion and thermophoresis effects leads the nanoparticles to move actively from the wall to the fluid which significantly enhances the temperature.

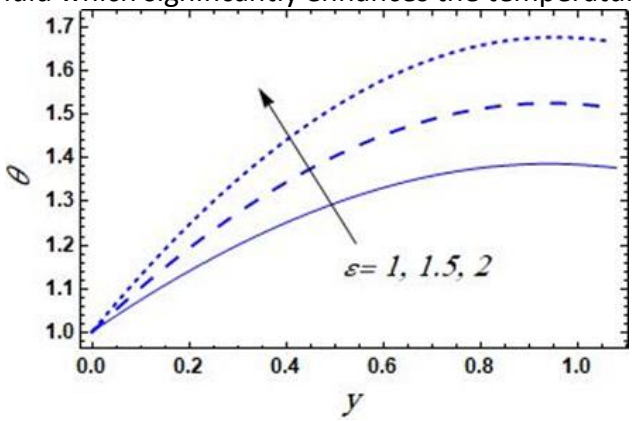

Fig. 5. Variation of ε on θ versus y

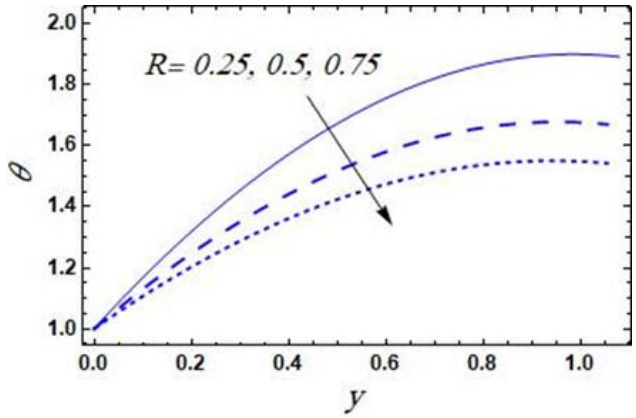

Fig. 6. Variation of R on θ versus y

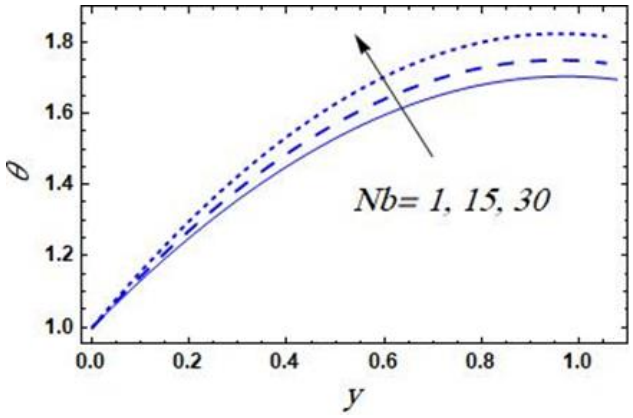

Fig. 7. Variation of Nb on θ versus y

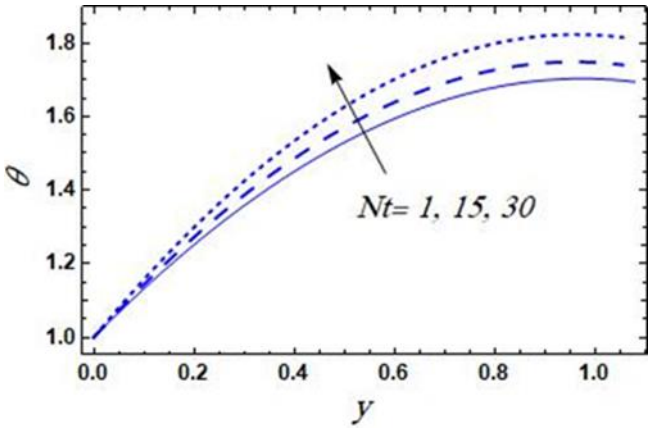

Fig. 8. Variation of Nt on θ versus y

Figure 9 and Figure 10, respectively, show how the nanoparticle concentration distribution ϕ behaves along the normal axis y for various values of the order reaction n and the chemical reaction parameter γ. These graphs depict that the concentration of nanoparticles ϕ grows as n increases, whereas it decreases by increasing the value of γ. Additionally, the variation of the nanoparticle concentration distribution ϕ for various values of n and γ become lower along the normal axis y and ends up with the lowest value near the right wall. It is clear that the lowest value of ϕ increases by increasing n, while it decreases as γ increases. We discovered that the influence of γ_3 and Sc on nanoparticle concentration distribution ϕ is comparable to those shown in Figure 10. These graphs are omitted here to save space.

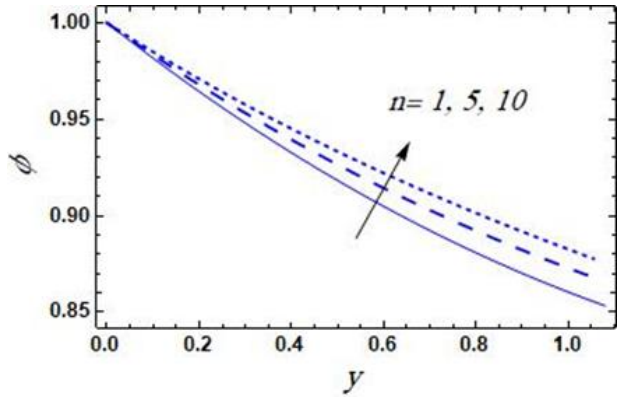

Fig. 9. Variation of n on ϕ versus y

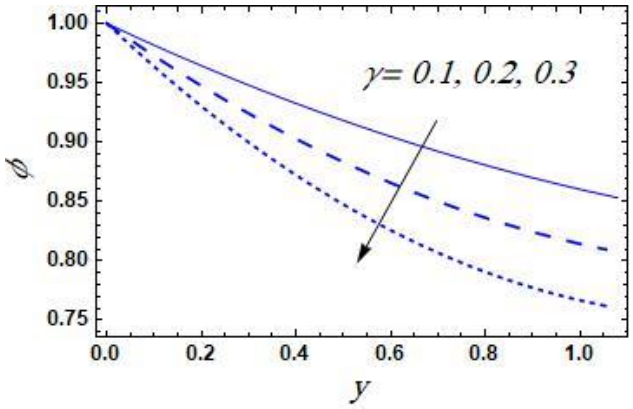

Fig. 10. Variation of γ on ϕ versus y

Figure 11 and Figure 12 show the behavior of skin friction coefficient τ_{xy} with Bingham number Bn and the velocity slip parameter β_1, respectively. It is clear from these figures that the skin friction coefficient τ_{xy} increases by increasing Bn, while it decreases as β_1 increasing. Furthermore, the relation between τ_{xy} and the parallel coordinate x seems to be a wavy relation, *i.e.,* τ_{xy} increases or decreases by increasing the parallel coordinate x. We have observed that the influence of $\gamma_1, \gamma_2, \gamma_3, M$ and m_1 is similar to e effect of Bn that is captured in Figure 11, while the effect of Gr, Gc and m is similar to the effect of β_1 that is given in Figure 12. But the obtained curves for γ_2, γ_3 and m are closer to each other comparing with the curves that obtained in Figure 11 and Figure 12. Note that these figures are not given here for want of space.

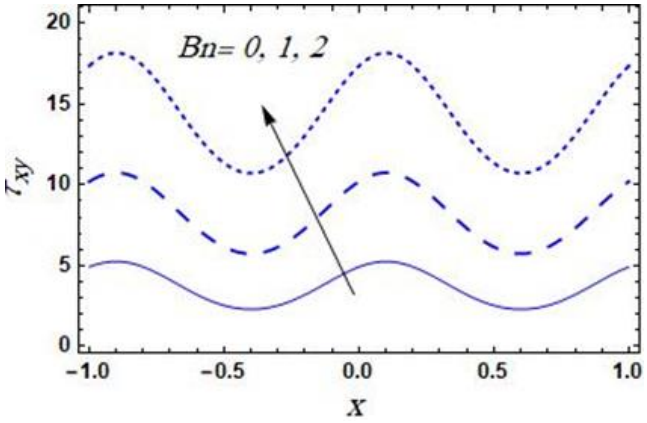

Fig. 11. Variation of Bn on τ_{xy} versus x

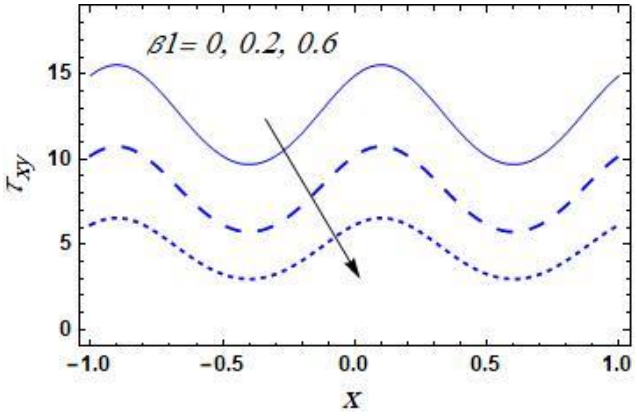

Fig. 12. Variation of β_1 on τ_{xy} versus x

The change in heat transfer coefficient $Z(x)$ with the parallel coordinate x for different values of radiation parameter R and Brinkman number Br at the right wall is displayed in Figure 13 and Figure 14, respectively. Actually, the rate of heat transfer or heat flux at the right wall of the channel is defined by the dimensionless expression for heat transfer coefficient $Z(x)$. An oscillatory behavior occurs in these figures between $Z(x)$ and x-axis due to the propagation of the peristaltic waves along the channel walls. Figure 13 shows that the absolute value of $Z(x)$ decreases with the increase of R, while it increases by increasing Br as captured in Figure 14. Also, we found that the influence of Bn, Nt, Nb, Pr, γ_2, ε and M on $Z(x)$ is identically similar to the effect of Br that is shown in Figure 14. Here, we excluded these figures to prevent any type of repetition.

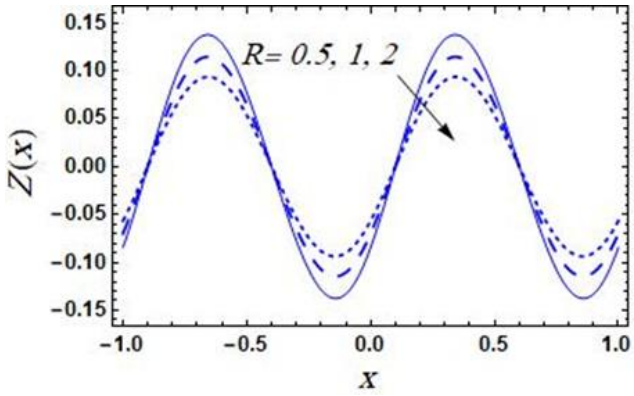

Fig. 13. Variation of R on $Z(x)$ versus x

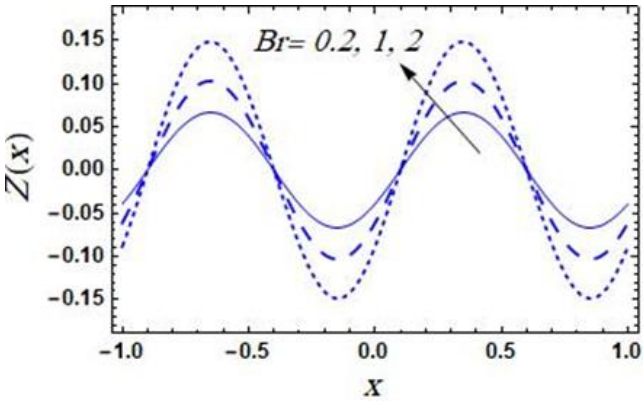

Fig. 14. Variation of Br on $Z(x)$ versus x

Figure 15 shows the behavior of Nusselt number Nu with Brinkman number Br for various values of the Hartman number M. Figure 16 depicts the behavior of Nusselt number Nu with the concentration slip parameter γ_3 for different values of the radiation parameter R. We noticed from these graphs that an increase of M, Br and γ_3 increases Nusselt number Nu, whereas Nu decreases as R increases. Moreover, the difference of Nusselt number for different values of M and R becomes greater with increasing Br and γ_3 and rises to the highest value at a specific value of Br and γ_3; exactly when $Br = \gamma_3 = 1$ as shown in Figure 15 and Figure 16. We also observed that the highest value of Nusselt number Nu rises by increasing Hartman number M as shown in Figure 15, while it decreases with the increase of the radiation parameter R as captured in Figure 16. Further, we observed that Nusselt number Nu increases by increasing each of Bn, Pr, ε and γ_3. Furthermore, we noticed that Nusselt number for different values of Bn and R becomes greater and rises to the highest value, but it becomes lower and falls to the lowest value for Pr, Br, Bn and γ_3. Here, the figures are not provided to save place. In Figure 15, we can observe a linear relation between Nu and M. Also, the curves are sound to be parallel to Br for a small value of M.

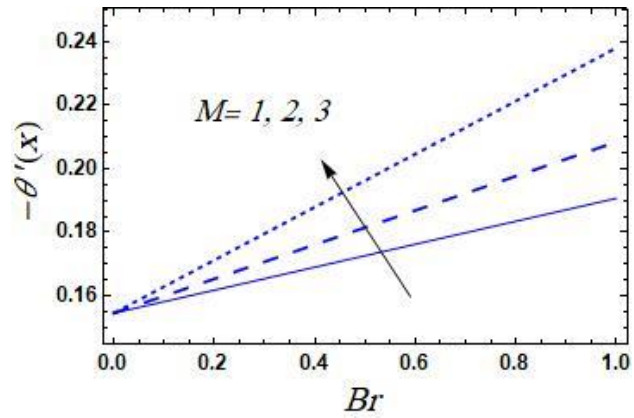

Fig. 15. Variation of M on Nu versus Br

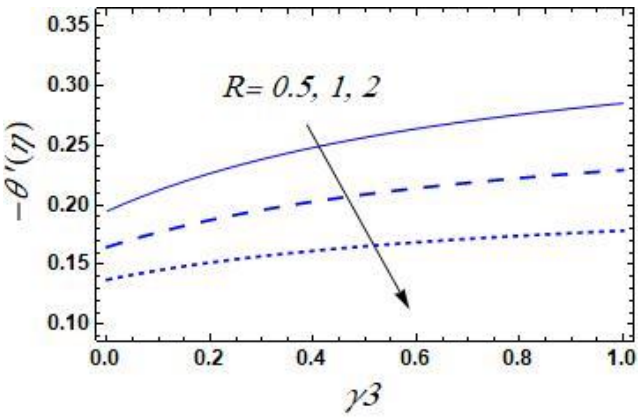

Fig. 16. Variation of R on Nu versus γ_3

The behavior of Sherwood number Sh with the chemical reaction parameter γ for several values of Schmidt number Sc and the concentration slip parameter γ_3 is presented in Figure 17 and Figure 18, respectively. These figures show that Sherwood number Sh decreases by increasing the values of Sc and γ, while it enhances by increasing the value of γ_3. The difference of the Sherwood number Sh for different values of Sc and γ_3 becomes lower by increasing γ and reaches the lowest value. Here, the lowest value of Sh decreases by increasing Sc, while it increases by increasing γ_3.

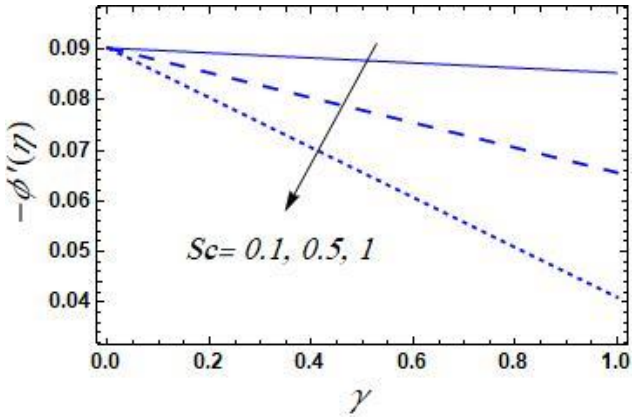

Fig. 17. Variation of Sc on Sh versus γ

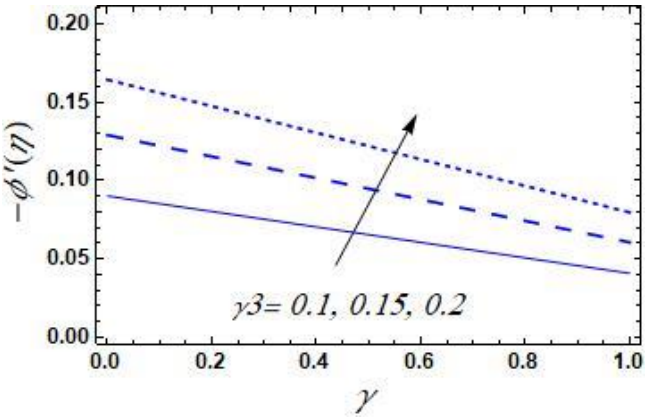

Fig. 18. Variation of γ_3 on Sh versus γ

Figure 19 and Figure 20 are obtained to investigate the sequences of the couple stress parameter γ_1 and the local mass Grashof number Gc on the entropy generation number Ns, respectively. Figure 19 exhibits that entropy generation number Ns increases by increasing the couple stress parameter γ_1, but it decreases with increasing Gc. Moreover, we noticed from Figure 19 and Figure 20 that the entropy generation number Ns becomes greater by increasing the normal axis y and arrives to the highest value, after which it decreases and then it starts to increase again near the right wall; approximately at $y = 0.7$. Here, the highest value of Ns increases with the increase of γ_1, while it decreases by increasing Gc. Further, we observed that the influence each of ε, M, Pr, Bn, m_1, Nt and Br on entropy generation number Ns is similar to the effect of γ_1 that is shown in Figure 19. Otherwise, we observed that the effect of Gr, β_1, R and Nb on entropy generation number Ns is similar to the effect of Gc that is captured in Figure 20.

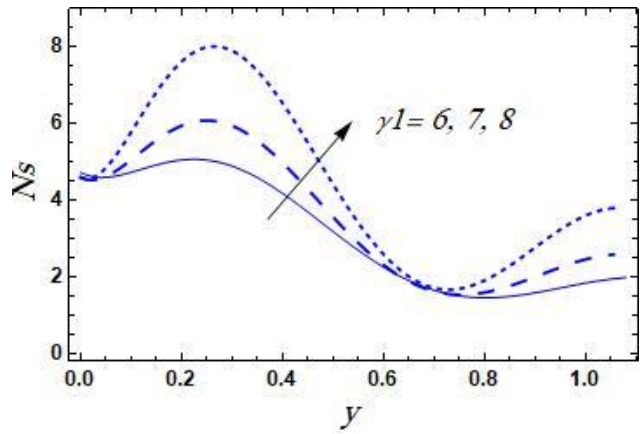

Fig. 19. Variation of $\gamma_1$on Nu versus y

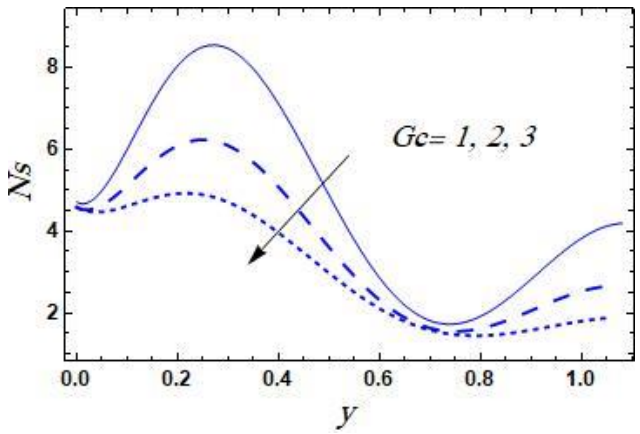

Fig. 20. Variation of Gc on Nu versus y

6. Conclusion

In this study we extend the work of Akbar *et al.,* [39] by including MHD Bingham plastic nanofluid in the present of Soret and Dufour effects, couple stresses and chemical reaction. Homotopy perturbation method (HPM) is employed to solve the system of nonlinear differential equations. Graphs for velocity, temperature and nanoparticle concentration distributions of interest parameter of the given problem are plotted. Graphical representations of the heat transfer coefficient, Nusselt number, Sherwood number and entropy generation number are plotted. This kind of flow has many applications in various fields [51-56]. Furthermore, physical explanations for

interest parameter of the presented problem are provided. The key findings can be summed up as follows

i. Increase each of m, m_1, γ_1 and Bn causes a decrease in the velocity u, while increase Br, R, Nt, Nb, Sc, Gr, Gc, γ, γ_2, γ_3, ε and M increase it.
ii. The velocity u increases by increasing β_1, but an opposite behavior occurs near the right wall of the channel; approximately at $y > 0.65$.
iii. By increasing the normal axis y, the velocity u for different values of m, m_1, Bn, Br, β_1, γ, γ_1, γ_2, γ_3, Sc, Gr, Gc, ε, R, Nt, Nb and M becomes lower to reach the minimum value, and then it increases near the right wall of the channel.
iv. Increase each of m, β_1, γ, γ_1, γ_2, γ_3, Sc, Gr, Gc and R causes a reduction of the temperature θ, while an enhancement occurs in θ by increasing each of m_1, Bn, Br, ε, Nb, Nt and M.
v. By increasing the normal axis y, the temperature θ for different values of m, m_1, β_1, Bn, Br, γ, γ_1, γ_2, γ_3, Sc, Gr, Gc, ε, R, Nb, Nt and M becomes greater and ends up with the maximum value at the right wall of the channel.
vi. While the nanoparticle concentration ϕ decreases by increasing each of Sc, γ, γ_3 and Sr, it increases with the increase of n.
vii. By increase the normal axis y, the nanoparticle concentration distribution ϕ for different values of Sc, γ, n and Sr becomes lower and ends up with the minimum value at the right wall of the channel.
viii. The skin friction coefficient τ_{xy} increases by increasing Bn, of γ_1, , γ_2, γ_3, M and m_1, while it decreases by increasing β_1, for Gr, Gc and m.
ix. Increasing R causes a reduction of the absolute value of heat transfer coefficient $Z(x)$, while an enhancement appears in $Z(x)$ by increasing each of Br, Bn, Nt, Nb, Pr, γ_2, ε and M.
x. Increasing R reduces Nusselt number Nu, while an increase of M, Bn, M, Pr, Br, M, ε and γ_3 enhances it.
xi. Nusselt number Nu for several values of M, Bn and R becomes greater and rises to the highest value, but it becomes lower and falls to the lowest value for Pr, Br, Bn and γ_3.
xii. Increasing Sc and γ decreases Sherwood number Sh , while increasing γ_3 enhances it.
xiii. Sherwood number Sh for several values of γ, γ_3 and Sc becomes lower to arrive to the minimum value.
xiv. Entropy generation number Ns enhances by increasing the value of γ_1, ε, M, Pr, Bn, m_1, Nt and Br, whereas it decreases reducing the values of Gc, Gr, β_1, R and Nb.
xv. The entropy generation number Ns becomes greater and gets to the maximum value, after which it decreases and then it starts to increase again near the right wall; approximately at $y = 0.7$.

References

[1] Eldabe, Nabil TM, Mohamed A. Hassan, and Mohamed Y. Abou-Zeid. "Wall properties effect on the peristaltic motion of a coupled stress fluid with heat and mass transfer through a porous medium." *Journal of engineering mechanics* 142, no. 3 (2016): 04015102. https://doi.org/10.1061/(ASCE)EM.1943-7889.0001029
[2] Abou-Zeid, Mohamed Y. "Homotopy perturbation method for couple stresses effect on MHD peristaltic flow of a non-Newtonian nanofluid." *Microsystem Technologies* 24, no. 12 (2018): 4839-4846. https://doi.org/10.1007/s00542-018-3895-1
[3] Alsaedi, A., Nasir Ali, Dharmendra Tripathi, and Tasawar Hayat. "Peristaltic flow of couple stress fluid through uniform porous medium." *Applied Mathematics and Mechanics* 35, no. 4 (2014): 469-480. https://doi.org/10.1007/s10483-014-1805-8

[4] Ramesh, K. "Effects of slip and convective conditions on the peristaltic flow of couple stress fluid in an asymmetric channel through porous medium." *computer methods and programs in biomedicine* 135 (2016): 1-14. https://doi.org/10.1016/j.cmpb.2016.07.001

[5] Ramesh, K. "Influence of heat and mass transfer on peristaltic flow of a couple stress fluid through porous medium in the presence of inclined magnetic field in an inclined asymmetric channel." *Journal of Molecular Liquids* 219 (2016): 256-271. https://doi.org/10.1016/j.molliq.2016.03.010

[6] Eldabe, N. T. M., G. Saddeck, and A. F. El-Sayed. "Heat transfer of MHD non-Newtonian Casson fluid flow between two rotating cylinders." *Mechanics and Mechanical Engineering* 5, no. 2 (2001): 237-251.

[7] Ouaf, Mahmoud Elhassan Mahmoud, and Mohamed Yahya Abou-zeid. "Electromagnetic and non-Darcian effects on a micropolar non-Newtonian fluid boundary-layer flow with heat and mass transfer." *International Journal of Applied Electromagnetics and Mechanics* 66, no. 4 (2021): 693-703. https://doi.org/10.3233/JAE-201623

[8] Eldabe, Nabil TM, and Mona AA Mohamed. "Heat and mass transfer in hydromagnetic flow of the non-Newtonian fluid with heat source over an accelerating surface through a porous medium." *Chaos, Solitons & Fractals* 13, no. 4 (2002): 907-917. https://doi.org/10.1016/S0960-0779(01)00066-2

[9] Eldabe, Nabil Tawfik, Galal M. Moatimid, Mohamed Abouzeid, Abdelhafeez A. El-Shekhipy, and Naglaa Fawzy Abdallah. "Instantaneous thermal-diffusion and diffusion-thermo effects on carreau nanofluid flow over a stretching porous sheet." *Journal of Advanced Research in Fluid Mechanics and Thermal Sciences* 72, no. 2 (2020): 142-157. https://doi.org/10.37934/arfmts.72.2.142157

[10] Mohamed, Mona AA, and Mohamed Y. Abou-zeid. "MHD peristaltic flow of micropolar Casson nanofluid through a porous medium between two co-axial tubes." *Journal of Porous Media* 22, no. 9 (2019). https://doi.org/10.1615/JPorMedia.2018025180

[11] Eldabe, Nabil T., Raafat R. Rizkalla, Mohamed Y. Abou-Zeid, and Vivian M. Ayad. "Effect of induced magnetic field on non-Newtonian nanofluid Al2O3 motion through boundary-layer with gyrotactic microorganisms." *Thermal Science* 26, no. 1 Part B (2022): 411-422. https://doi.org/10.2298/TSCI200408189E

[12] Eldabe, N. T., M. Y. Abou-zeid, AS Abo Seliem, A. A. Elenna, and N. Hegazy. "Thermal Diffusion and Diffusion Thermo Effects on Magnetohydrodynamics Transport of Non-Newtonian Nanofluid Through a Porous Media Between Two Wavy Co-Axial Tubes." *IEEE Transactions on Plasma Science* 50, no. 5 (2022): 1282-1290. https://doi.org/10.1109/TPS.2022.3161740

[13] Eldabe, Nabil T., Sami M. El Shabouri, Tarek N. Salama, and Aya M. Ismael. "Ohmic and viscous dissipation effects on micropolar non-Newtonian nanofluid Al 2O 3 flow through a non-Darcy porous media." *International Journal of Applied Electromagnetics and Mechanics* Preprint (2022): 1-13. https://doi.org/10.3233/JAE-210100

[14] Abou-Zeid, Mohamed Y. "Implicit homotopy perturbation method for MHD non-Newtonian nanofluid flow with Cattaneo-Christov heat flux due to parallel rotating disks." *Journal of Nanofluids* 8, no. 8 (2019): 1648-1653. https://doi.org/10.1166/jon.2019.1717

[15] Eldabe, Nabil T., Raafat R. Rizkalla, Mohamed Y. Abouzeid, and Vivian M. Ayad. "Thermal diffusion and diffusion thermo effects of Eyring-Powell nanofluid flow with gyrotactic microorganisms through the boundary layer." *Heat Transfer—Asian Research* 49, no. 1 (2020): 383-405. https://doi.org/10.1002/htj.21617

[16] Eldabe, Nabil Tawfik, Samy M. El Shaboury, Hassan A. El Arabawy, Mohamed Y. Abou-zeid, and Alaa Abuiyada. "Wall properties and Joule heating effects on MHD peristaltic transport of Bingham non-Newtonian nanofluid." *International Journal of Applied Electromagnetics and Mechanics* Preprint (2022): 1-20. https://doi.org/10.3233/JAE-210126

[17] Eldabe, Nabil TM, Mohamed Y. Abou-Zeid, M. E. Ouaf, D. R. Mustafa, and Y. M. Mohammed. "Cattaneo–Christov heat flux effect on MHD peristaltic transport of Bingham Al 2 O 3 nanofluid through a non–Darcy porous medium." *International Journal of Applied Electromagnetics and Mechanics* 68 (2022): 59-84. https://doi.org/10.3233/JAE-210057

[18] Eldabe, Nabil Tawfik, Mohamed Abouzeid, and Hamida A. Shawky. "MHD peristaltic transport of Bingham blood fluid with heat and mass transfer through a non-uniform channel." *Journal of Advanced Research in Fluid Mechanics and Thermal Sciences* 77, no. 2 (2021): 145-159. https://doi.org/10.37934/arfmts.77.2.145159

[19] Ismael, Aya, Nabil Tawfik Eldabe, Mohamed Abouzeid, and Sami Elshabouri. "Entropy generation and nanoparticles Cu O effects on MHD peristaltic transport of micropolar non-Newtonian fluid with velocity and temperature slip conditions." *Egyptian Journal of Chemistry* 65, no. 9 (2022): 715-722.

[20] Ibrahim, Mohamed, Naglaa Abdallah, and Mohamed Abouzeid. "Activation energy and chemical reaction effects on MHD Bingham nanofluid flow through a non-Darcy porous media." *Egyptian Journal of Chemistry* (2022).. https://doi.org/10.21608/ejchem.2022.117814.5310

[21] Eldabe, Nabil T., Mohamed Y. Abou-zeid, Adel Abosaliem, Ahmed Elenna, and Nada Hegazy. "Homotopy perturbation approach for Ohmic dissipation and mixed convection effects on non-Newtonian nanofluid flow

between two co-axial tubes with peristalsis." *International Journal of Applied Electromagnetics and Mechanics* 67, no. 2 (2021): 153-163. https://doi.org/10.3233/JAE-210001

[22] Mustafa, M., S. Hina, T. Hayat, and A. Alsaedi. "Slip effects on the peristaltic motion of nanofluid in a channel with wall properties." *Journal of heat transfer* 135, no. 4 (2013). https://doi.org/10.1115/1.4023038

[23] Eldabe, Nabil, Mohamed Abouzeid, and Hemat Ali. "Effect of heat and mass transfer on casson fluid flow between two co-axial tubes with peristalsis." *Journal of Advanced Research in Fluid Mechanics and Thermal Sciences* 76, no. 1 (2020): 54-75. https://doi.org/10.37934/arfmts.76.1.5475

[24] Eldabe, Nabil, and Mohamed Abou-Zeid. "Radially varying magnetic field effect on peristaltic motion with heat and mass transfer of a non-Newtonian fluid between two co-axial tubes." *Thermal Science* 22, no. 6 Part A (2018): 2449-2458. https://doi.org/10.2298/TSCI160409292E

[25] Mansour, Hesham Mohamed, and Mohamed Y. Abou-zeid. "Heat and mass transfer effect on non-Newtonian fluid flow in a non-uniform vertical tube with peristalsis." *Journal of Advanced Research in Fluid Mechanics and Thermal Sciences* 61, no. 1 (2019): 44-62.

[26] Abou-zeid, Mohamed Y., and Mona AA Mohamed. "Homotopy perturbation method for creeping flow of non-Newtonian power-law nanofluid in a nonuniform inclined channel with peristalsis." *Zeitschrift für Naturforschung A* 72, no. 10 (2017): 899-907. https://doi.org/10.1515/zna-2017-0154

[27] El-dabe, Nabil T., Mohamed Y. Abou-zeid, Mona A. Mohamed, and Mohamed Maged. "Peristaltic flow of Herschel Bulkley nanofluid through a non-Darcy porous medium with heat transfer under slip condition." *International Journal of Applied Electromagnetics and Mechanics* 66, no. 4 (2021): 649-668. https://doi.org/10.3233/JAE-201600

[28] Eldabe, N. T., G. M. Moatimid, M. Y. Abouzeid, A. A. ElShekhipy, and Naglaa F. Abdallah. "A semianalytical technique for MHD peristalsis of pseudoplastic nanofluid with temperature-dependent viscosity: Application in drug delivery system." *Heat Transfer—Asian Research* 49, no. 1 (2020): 424-440. https://doi.org/10.1002/htj.21619

[29] El-Dabe, Nabil, Mohamed Y. Abou-Zeid, Mona AA Mohamed, and Mohamed M. Abd-Elmoneim. "MHD peristaltic flow of non-Newtonian power-law nanofluid through a non-Darcy porous medium inside a non-uniform inclined channel." *Archive of Applied Mechanics* 91, no. 3 (2021): 1067-1077. https://doi.org/10.1007/s00419-020-01810-3

[30] Eldabe, Nabil T., Mohamed Y. Abou-Zeid, Omar H. El-Kalaawy, Salah M. Moawad, and Ola S. Ahmed. "Electromagnetic steady motion of Casson fluid with heat and mass transfer through porous medium past a shrinking surface." *Thermal Science* 25, no. 1 Part A (2021): 257-265. https://doi.org/10.2298/TSCI190418416E

[31] Ouaf, Mahmoud E., Mohamed Abou-zeid, and Yasmeen M. Younis. "Entropy generation and chemical reaction effects on MHD non-Newtonian nanofluid flow in a sinusoidal channel." *International Journal of Applied Electromagnetics and Mechanics* Preprint (2022): 1-21. https://doi.org/10.3233/JAE-210215

[32] El-Dabe, Nabil, Abeer A. Shaaban, Mohamed Y. Abou-Zeid, and Hemat A. Ali. "Magnetohydrodynamic non-Newtonian nanofluid flow over a stretching sheet through a non-Darcy porous medium with radiation and chemical reaction." *Journal of Computational and Theoretical Nanoscience* 12, no. 12 (2015): 5363-5371. https://doi.org/10.1166/jctn.2015.4528

[33] Eldabe, Nabil Tawfik, Galal M. Moatimid, Mohamed Abouzeid, Abdelhafeez A. Elshekhipy, and Naglaa Fawzy Abdallah. "Semi-analytical treatment of Hall current effect on peristaltic flow of Jeffery nanofluid." *International Journal of Applied Electromagnetics and Mechanics* 67, no. 1 (2021): 47-66. https://doi.org/10.3233/JAE-201626

[34] El-dabe, Nabil Tawfik, Mohamed Yahya Abou-zeid, and Ola S. Ahmed. "Motion of a thin film of a fourth grade nanofluid with heat transfer down a vertical cylinder: Homotopy perturbation method application." *Journal of Advanced Research in Fluid Mechanics and Thermal Sciences* 66, no. 2 (2020): 101-113.

[35] Asghar, S., Q. Hussain, T. Hayat, and F. Alsaadi. "Hall and ion slip effects on peristaltic flow and heat transfer analysis with Ohmic heating." *Applied Mathematics and Mechanics* 35, no. 12 (2014): 1509-1524. https://doi.org/10.1007/s10483-014-1881-6

[36] Nowar, Khalid. "Peristaltic flow of a nanofluid under the effect of Hall current and porous medium." *Mathematical Problems in Engineering* 2014 (2014). https://doi.org/10.1155/2014/389581

[37] Elshehawey, E. F., N. T. Eldabe, E. M. Elbarbary, and Nasser S. Elgazery. "Chebyshev finite-difference method for the effects of Hall and ion-slip currents on magneto-hydrodynamic flow with variable thermal conductivity." *Canadian Journal of Physics* 82, no. 9 (2004): 701-715. https://doi.org/10.1139/p04-038

[38] Abbasi, F. M., T. Hayat, and A. Alsaedi. "Numerical analysis for MHD peristaltic transport of Carreau–Yasuda fluid in a curved channel with Hall effects." *Journal of Magnetism and Magnetic Materials* 382 (2015): 104-110. https://doi.org/10.1016/j.jmmm.2015.01.040

[39] Akbar, Y., F. M. Abbasi, and S. A. Shehzad. "Thermal radiation and Hall effects in mixed convective peristaltic transport of nanofluid with entropy generation." *Applied Nanoscience* 10, no. 12 (2020): 5421-5433. https://doi.org/10.1007/s13204-020-01446-3

[40] Hayat, Tasawar, Sabia Asghar, Anum Tanveer, and Ahmed Alsaedi. "Outcome of slip features on the peristaltic flow of a Prandtl nanofluid with inclined magnetic field and chemical reaction." *The European Physical Journal Plus* 132, no. 5 (2017): 1-16. https://doi.org/10.1140/epjp/i2017-11486-8

[41] Bhatti, M. M., and M. M. Rashidi. "Study of heat and mass transfer with Joule heating on magnetohydrodynamic (MHD) peristaltic blood flow under the influence of Hall effect." *Propulsion and Power Research* 6, no. 3 (2017): 177-185. https://doi.org/10.1016/j.jppr.2017.07.006

[42] Patel, S. A., and R. P. Chhabra. "Heat transfer in Bingham plastic fluids from a heated elliptical cylinder." *International Journal of Heat and Mass Transfer* 73 (2014): 671-692. https://doi.org/10.1016/j.ijheatmasstransfer.2014.02.024

[43] Papanastasiou, Tasos C. "Flows of materials with yield." *Journal of rheology* 31, no. 5 (1987): 385-404. https://doi.org/10.1122/1.549926

[44] Papanastasiou, T. C., and A. G. Boudouvis. "Flows of viscoplastic materials: models and computations." *Computers & Structures* 64, no. 1-4 (1997): 677-694. https://doi.org/10.1016/S0045-7949(96)00167-8

[45] Hayat, Tasawar, Maryam Shafique, Anum Tanveer, and Ahmed Alsaedi. "Radiative peristaltic flow of Jeffrey nanofluid with slip conditions and Joule heating." *PloS one* 11, no. 2 (2016): e0148002. https://doi.org/10.1371/journal.pone.0148002

[46] Abou-zeid, Mohamed Y. "Magnetohydrodynamic boundary layer heat transfer to a stretching sheet including viscous dissipation and internal heat generation in a porous medium." *Journal of porous Media* 14, no. 11 (2011). https://doi.org/10.1615/JPorMedia.v14.i11.50

[47] Abou-Zeid, Mohamed. "Homotopy perturbation method to MHD non-Newtonian nanofluid flow through a porous medium in eccentric annuli with peristalsis." *Thermal Science* 21, no. 5 (2017): 2069-2080. https://doi.org/10.2298/TSCI150215079A

[48] Abou-Zeid, M. Y. "Homotopy perturbation method to gliding motion of bacteria on a layer of power-law nanoslime with heat transfer." *Journal of Computational and Theoretical Nanoscience* 12, no. 10 (2015): 3605-3614. https://doi.org/10.1166/jctn.2015.4246

[49] Eldabe, Nabil T., and Mohamed Y. Abou-zeid. "Magnetohydrodynamic peristaltic flow with heat and mass transfer of micropolar biviscosity fluid through a porous medium between two co-axial tubes." *Arabian Journal for Science and Engineering* 39, no. 6 (2014): 5045-5062. https://doi.org/10.1007/s13369-014-1039-1

[50] Abou-zeid, Mohamed Y., and Mahmoud E. Ouaf. "Hall currents effect on squeezing flow of non-Newtonian nanofluid through a porous medium between two parallel plates." *Case Studies in Thermal Engineering* 28 (2021): 101362. https://doi.org/10.1016/j.csite.2021.101362

[51] Beleri, Joonabi, and Asha S. Kotnurkar. "Peristaltic Transport of Ellis Fluid under the Influence of Viscous Dissipation Through a Non-Uniform Channel by Multi-Step Differential Transformation Method." *Journal of Advanced Research in Numerical Heat Transfer* 9, no. 1 (2022): 1-18.

[52] Ab Rahman, Rosdi, Mahmod Abd Hakim Mohamad, Masiri Kaamin, Mohd Faizal Mohideen Batcha, Mohammad Daniel Aiman Mazlan, Muhammad Luqman Rosli, and Mohamad Azrul Arif Che Aziz. "Experimental study of Peltier-Based Thermoelectric Cooling Box System." *Journal of Advanced Research in Applied Mechanics* 94, no. 1 (2022): 1-6.

[53] Khan, Ansab Azam, Khairy Zaimi, Suliadi Firdaus Sufahani, and Mohammad Ferdows. "MHD flow and heat transfer of double stratified micropolar fluid over a vertical permeable shrinking/stretching sheet with chemical reaction and heat source." *Journal of Advanced Research in Applied Sciences and Engineering Technology* 21, no. 1 (2020): 1-14. https://doi.org/10.37934/araset.21.1.114

[54] Sharafatmandjoor, Shervin. "Effect of Imposition of viscous and thermal forces on Dynamical Features of Swimming of a Microorganism in nanofluids." *Journal of Advanced Research in Micro and Nano Engineering* 8, no. 1 (2022): 1-8.

[55] Akaje, Wasiu, and B. I. Olajuwon. "Impacts of Nonlinear thermal radiation on a stagnation point of an aligned MHD Casson nanofluid flow with Thompson and Troian slip boundary condition." *Journal of Advanced Research in Experimental Fluid Mechanics and Heat Transfer* 6, no. 1 (2021): 1-15.

[56] Mahat, Rahimah, Muhammad Saqib, Imran Ulah, Sharidan Shafie, and Sharena Mohamad Isa. "MHD Mixed Convection of Viscoelastic Nanofluid Flow due to Constant Heat Flux." *Journal of Advanced Research in Numerical Heat Transfer* 9, no. 1 (2022): 19-25.